PHYSICAL REVIEW A **83**, 021605(R) (2011)

Mapping out the quasicondensate transition through the dimensional crossover from one to three dimensions

J. Armijo,[1] T. Jacqmin,[1] K. Kheruntsyan,[2] and I. Bouchoule[1]
[1]*Laboratoire Charles Fabry, UMR 8501 du CNRS, Institut d'Optique, F-91127 Palaiseau Cedex, France*
[2]*ARC Centre of Excellence for Quantum-Atom Optics, School of Physical Sciences, University of Queensland, Brisbane, Queensland 4072, Australia*
(Received 12 November 2010; published 25 February 2011)

By measuring the density fluctuations in a highly elongated weakly interacting Bose gas, we observe and quantify the transition from the ideal gas to a quasicondensate regime throughout the dimensional crossover from a purely one-dimensional (1D) to an almost three-dimensional (3D) gas. We show that that the entire transition region and the dimensional crossover are described surprisingly well by the modified Yang-Yang model. Furthermore, we find that at low temperatures the linear density at the quasicondensate transition scales according to an *interaction-driven* scenario of a longitudinally uniform 1D Bose gas, whereas at high temperatures it scales according to the *degeneracy-driven* critical scenario of transverse condensation of a 3D ideal gas.

DOI: 10.1103/PhysRevA.83.021605 PACS number(s): 03.75.Hh, 67.10.Ba

Low-dimensional (one- or two-dimensional) systems can have physical properties dramatically different from their three-dimensional (3D) counterparts. Experimental realizations of such systems in recent years has been particularly exciting in the field of ultracold atomic gases [1,2]. Here, the reduction of dimensionality is achieved by using highly anisotropic trapping potentials, where lowering the temperature leads to "freezing" out certain motional degrees of freedom to the respective ground state. For situations when the freezing is not perfect, an intriguing fundamental question arises: How does the low-dimensional and 3D physics get reconciled in the dimensional crossover?

In this paper we address this question for a weakly interacting Bose gas that is confined transversely by a harmonic trap of frequency $\omega_\perp/2\pi$ but is homogeneous in the thermodynamic limit with respect to the longitudinal direction. The one-dimensional (1D) regime is obtained when the thermal energy k_BT and the chemical potential μ become much smaller than the transverse excitation energy $\hbar\omega_\perp$. In the absence of interatomic interactions, the homogeneous 1D gas is characterized by the absence of Bose-Einstein condensation. In the 3D limit, however, for $k_BT \gg \hbar\omega_\perp$, a sharp *transverse condensation* is expected: The atoms accumulate in the transverse ground state due to the saturation of population in the transversally excited states, yet the resulting 1D gas is still uncondensed with respect to the longitudinal states [3]. By incorporating weak repulsive interactions, in the 1D limit one expects a smooth *interaction-driven* transition from the ideal-gas regime toward the so-called quasicondensate regime [4] characterized by suppressed density fluctuations while the phase still fluctuates. Quasicondensates can be also created in the 3D limit [5], as observed experimentally [6,7]. In this paper we investigate the nature of the quasicondensate transition throughout the whole 1D–3D dimensional crossover.

Our study relies on the measurement of atomic density fluctuations, previously used to identify the two limiting regimes—the ideal gas and the quasicondensate [8]. Owing to a higher measurement precision, we now probe the transition itself, including the crossover from a deeply 1D regime with $k_BT \ll \hbar\omega_\perp$ to an almost 3D regime with $k_BT \simeq 3\hbar\omega_\perp$. For our parameters, the chemical potential becomes non-negligible compared to $\hbar\omega_\perp$ only in the quasicondensate regime so that the dimensional crossover occurring in the quasicondensate transition is relative only to T. Although the atoms in our experiment are trapped longitudinally, we probe the physics of a longitudinally *homogeneous* gas because the longitudinal confinement is sufficiently weak and the density fluctuations are measured locally. We find that the transition in the entire dimensional crossover is well described by the so-called modified Yang-Yang model (MYYM) [9], in which the atoms in the transverse ground state are treated using the exact thermodynamic solution of the 1D Bose-gas model with contact interactions [10], whereas the atoms in the transverse excited states are treated as independent ideal 1D Bose gases. This shows that the quasicondensate transition maintains its 1D physical origin even for temperatures $k_BT > \hbar\omega_\perp$. Moreover, by monitoring the linear density at the quasicondensation transition, we show that the physics is continuously modified across the dimensional crossover. In the 1D regime, the transition is broad and interaction-driven, and it scales as expected from the theory of weakly interacting gases. In the 3D limit, the transition is ruled by the ideal-gas scenario of transverse condensation and the transition density no longer depends on the interaction strength. We give a theoretical prediction for the temperature of this dimensional crossover, $T_{\rm DC}$, and show that, unless the interactions are extremely weak, $k_BT_{\rm DC} \sim \hbar\omega_\perp$. Dimensional crossover in other ultracold gas systems has been studied both theoretically [11–14] and experimentally [15,16], but without comparison continuously throughout the crossover.

We conduct our experiment on an atom chip using ^{87}Rb atoms in the $|F = 2, m_F = 2\rangle$ hyperfine state. The on-chip current-carrying microwires realize an Ioffe magnetic trap with a longitudinal oscillation frequency ranging from 5.0 to 8 Hz and a transverse oscillation frequency ranging from 3 to 4 kHz. An ultracold gas in thermal equilibrium is prepared using rf forced evaporation. We then take *in situ* absorption images of the atomic cloud using a nearly resonant laser at $\lambda = 780$ nm, as detailed in [17]. The imaging spatial resolution in the object plane has an rms width of about 2 μm, whereas

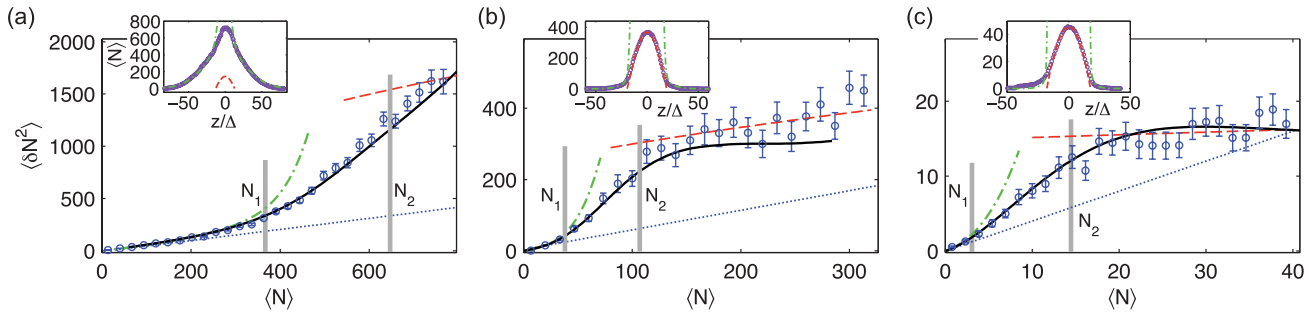

FIG. 1. (Color online) Density fluctuations across the quasicondensate transition, for $k_BT/\hbar\omega_\perp$ values of (a) 3.6, (b) 1.0, and (c) 0.09. The measured atom-number variances in individual pixels, $\langle \delta N^2 \rangle$, as a function of the mean atom number $\langle N \rangle$ are shown as circles, with the error bars representing the statistical uncertainty. Different curves denote the predictions from theoretical models, rescaled by the resolution factor $\kappa = 0.53$, 0.55, and 0.4 for (a), (b), and (c), respectively (see text): modified Yang-Yang model (solid), ideal Bose-gas (dashed-dotted), quasicondensate (dashed), and the Poissonian shot-noise level (dotted). The two vertical gray lines give the atom numbers $N_1 = \Delta n_1$ and $N_2 = \Delta n_2$ (see text). The insets show the average density profiles, together with the predictions from the same models (with different curves as in the main graphs). The chemical potential μ_0 in the trap center is deduced from the fit of the wings of the density profile to the ideal Bose-gas EoS for (a), and from the peak density and the quasicondensate EoS for (b) and (c). The trap oscillation frequencies are $\omega_\perp/2\pi = 3.0$ kHz, $\omega_\parallel/2\pi = 8.0(5)$ Hz for (a) and (b) and $\omega_\perp/2\pi = 3.9$ kHz, $\omega_\parallel/2\pi = 4.0(5)$ Hz for (c). The absolute temperatures T are (a) 510 nK , (b) 160 nK , and (c) 18 nK.

the camera pixel size is $\Delta = 4.5$ μm. By summing over the transverse pixels, we derive from the images the longitudinal atomic density profile, thus reducing the notion of a pixel to a segment of length Δ. The absolute calibration of the density profiles is described in [17]. We perform a statistical analysis of hundreds of images, taken under the same experimental conditions: For each density profile and pixel, we extract the atom number fluctuation $\delta N = N - \langle N \rangle$, where N is the measured number of atoms in the pixel and $\langle N \rangle$ its mean value. The fluctuations are binned according to $\langle N \rangle$ and the variance $\langle \delta N^2 \rangle$ is computed for each bin. Finally, we subtract the contribution of the optical shot noise, which is typically less than 20% of the atomic fluctuations. Figure 1 shows typical results for $\langle \delta N^2 \rangle$ for three different temperatures, together with the respective average density profiles. As the images are blurred due to finite imaging resolution, the measured fluctuations are reduced by a factor κ compared to their true values. We deduce κ from the measurement of atom number *correlations* between the adjacent pixels, as explained in [17].

For our experimental parameters, we can use the local density approximation along the longitudinal dimension z [18], since the correlation length l_c of density fluctuations, the pixel length Δ, and the cloud length L satisfy $l_c \ll \Delta \ll L$. Thus the gas contained in a pixel $[z, z+\Delta]$ is well described by a longitudinally homogeneous system in the thermodynamic limit, whose local chemical potential is $\mu(z) = \mu_0 - V(z)$, where $V(z)$ is the longitudinal trapping potential. The thermodynamic quantities can be derived from the equation of state (EoS) $n = n(\mu, T)$ for a longitudinally homogeneous, but transversely trapped gas, where n is the linear (1D) density. In particular, $\langle N \rangle = n\Delta$ and the atom-number fluctuations can be calculated using the thermodynamic relation

$$\langle \delta N^2 \rangle = k_B T \Delta (\partial n/\partial \mu)_T. \tag{1}$$

Thermometry is done in two alternative ways. For hot gases [as in Fig. 1(a)], assuming a perfectly harmonic longitudinal potential, we deduce T by fitting the wings of the density profile to the EoS of an ideal Bose gas,

$$n = \frac{1}{\lambda_T} \sum_{\alpha=1}^{\infty} \frac{e^{\alpha\mu/k_BT}}{\sqrt{\alpha}} \frac{1}{(1 - e^{-\alpha\hbar\omega_\perp/k_BT})^2}. \tag{2}$$

Here, $\lambda_T = \sqrt{2\pi\hbar^2/mk_BT}$ is the thermal de Broglie wavelength, and the EoS is obtained by summing the contributions of the transverse harmonic oscillator modes.

For the coldest samples, because of the lack of pixels in the ideal-gas part of the cloud, we deduce the temperature from the measured fluctuations in the quasicondensate (central) part, using Eq. (1) and the quasicondensate EoS [19],

$$\mu = \hbar\omega_\perp(\sqrt{1 + 4na} - 1), \tag{3}$$

valid in the entire 1D–3D crossover region with respect to μ, where $a = 5.7$ nm is the 3D scattering length. This fluctuation-based thermometry has an accuracy of about 20%, representing a viable alternative to thermometry based on the analysis of density ripples appearing after time of flight [20]. A related fluctuation-based thermometry [21,22] uses the knowledge of the longitudinal confining potential to deduce the gas compressibility $\partial n/\partial\mu$ from the density profiles. Although less general because of the assumption of validity of Eq. (3), our method has the advantage of working in not perfectly characterized longitudinal potentials, as is often the case in atom-chip experiments [9,23].

Once κ and T are determined, the measured atom number fluctuations are compared with different theoretical models without any further adjustable parameters. As we see from Fig. 1, the two main regimes of a weakly interacting Bose gas [18,24] are clearly identified. First, at low $\langle N \rangle$ the fluctuations follow the prediction from the ideal-gas EoS (2) (dashed-dotted curve). Within this regime, but for nondegenerate samples, the fluctuations are Poissonian and follow the shot-noise (dotted) line, as in Fig. 1(a) for $\langle N \rangle < 200$. For degenerate samples (in the quantum decoherent subregime [18,24]), atomic bunching due to Bose statistics raises the fluctuations well above the shot-noise level

[8,25]. The second main regime is the quasicondensate regime, where density fluctuations are suppressed by the repulsive interactions. The data in Fig. 1 indeed converge at large $\langle N\rangle$ toward the prediction of the quasicondensate EoS (3) (dashed lines).

To describe the transition between the two main regimes, we use the modified Yang-Yang model [9], whose EoS is

$$n = n_{YY}(\mu,T) + \sum_{j=1}^{\infty}(j+1)n_e(\mu_j,T). \tag{4}$$

Here, the first term describes the atoms in the transverse ground state treated within the exact thermodynamic solution of the 1D Bose-gas model [10], while the second term describes the atoms in the transverse excited states, each treated as an ideal Bose gas with a shifted chemical potential $\mu_j = \mu - j\hbar\omega_\perp$ and a linear density $n_e(\mu_j,T) = g_{1/2}(e^{\mu_j/k_BT})/\lambda_T$, where $g_{1/2}$ is a Bose function. Since $a \ll l_\perp$ in our experiment, where $l_\perp = \sqrt{\hbar/m\omega_\perp}$ is the transverse oscillator length, we use $g = 2\hbar\omega_\perp a$ [26] as the effective 1D coupling in the MYYM.

The transition to the quasicondensate state in a 1D gas occurs when the chemical potential crosses zero [27], over a width $\mu_t = (mg^2/\hbar^2)^{1/3}(k_BT)^{2/3}$ [25]. Neglecting correlations between the different transverse states, one can expect the excited state 1D gases to remain nearly ideal and hence the MYYM to correctly describe the quasicondensate transition as long as $\mu_t \ll \hbar\omega_\perp$, or $\mu_t/\hbar\omega_\perp = [(k_BT/\hbar\omega_\perp)(a/l_\perp)]^{2/3} \ll 1$. Since $a/l_\perp \simeq 0.03$ in our experiment, the MYYM can be expected to be valid up to temperatures significantly larger than $\hbar\omega_\perp/k_B$. The experimental data in Fig. 1 are indeed in remarkable agreement with the MYYM prediction in the entire transition region and for all explored temperatures.

In the quasicondensate regime, however, the MYYM underestimates the fluctuations at high densities. Indeed, when μ is no longer negligible compared to $\hbar\omega_\perp$, the repulsive interactions produce transverse swelling of the density profile—an effect not taken into account in the MYYM. This effect, which is a manifestation of the dimensional crossover with respect to μ [15], is, on the other hand, captured by the EoS (3), which better describes the quasicondensate regime [see Fig. 1(b), and also in [17] Fig. 2(b)].

To quantify the quasicondensate transition we define the linear densities n_1 and n_2 for which the measured fluctuations are 20% lower than the predictions of Eqs. (2) and (3), respectively. Plotting n_1 and n_2 against $k_BT/\hbar\omega_\perp$ (see Fig. 2) maps out the phase diagram and reveals the dimensional crossover as explained in the following.

In the 1D limit, $k_BT/\hbar\omega_\perp \ll 1$, the quasicondensate transition is expected to occur for a degenerate gas around the density [24,27]

$$n_t \simeq [m(k_BT)^2/\hbar^2 g]^{1/3}. \tag{5}$$

This estimate can be obtained by considering the EoS of a highly degenerate ideal Bose gas $n \simeq \sqrt{m(k_BT)^2/2\hbar^2|\mu|}$ [28], and requiring that $|\mu|$ becomes of the order of the interaction energy gn. In the low-temperature (1D) part of the phase diagram, we have fitted the right-hand side of Eq. (5) to both the n_1 and n_2 curves, with two different prefactors, $\alpha = 0.28$ and 1.1, respectively. As we can see, the experimental data and the MYYM follow the scaling law of Eq. (5) quite well in this part of the diagram. In contrast, the scaling law of the 1D degeneracy condition, $n_d = 1/\lambda_T$, does not account for the observed data, which implies that the quasicondensate transition is governed by interactions and not by degeneracy. Note that the transition begins for a gas that is not highly degenerate, which is a sign that the data are lying close to the crossover toward the strongly interacting regime and which explains why the quantum decoherent subregime barely exists in Figs. 1(b) and 1(c).

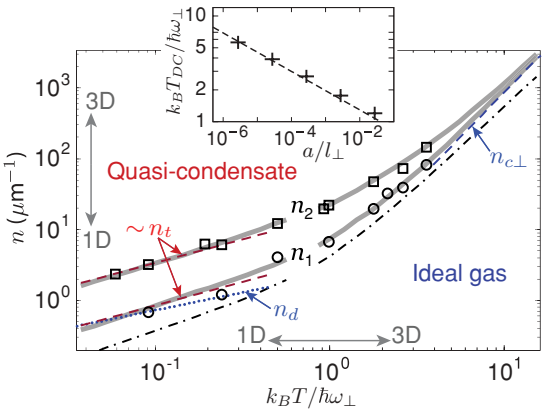

FIG. 2. (Color online) Phase diagram for the 1D–3D crossover. The data at $k_BT/\hbar\omega_\perp < 0.8$ (>0.8 kHz) are taken with $\omega_\perp/2\pi =$ 3.9 kHz (=3.0 kHz). The measured transition boundaries n_1 (circles) and n_2 (squares) are plotted along with the predictions from the MYYM (solid gray curves). The dashed-dotted curve is the perturbative calculation of n_1; all other lines are as labeled (see text). The inset shows the dimensional crossover temperature T_{DC} vs $a/l_\perp$ (crosses), fitted with a power law $(a/l_\perp)^{-2/11}$ (dashed line).

In the 3D limit, $k_BT/\hbar\omega_\perp \gg 1$, n_1 converges toward the linear density $n_{c\perp}$ corresponding to the the ideal-gas scenario of *transverse condensation*. This occurs when the peak 3D density ρ_0 reaches the threshold $\rho_0 \approx 2.612/\lambda_T^3$, giving [29]

$$n_{c\perp} = g_{5/2}(1)(k_BT/\hbar\omega_\perp)^2/\lambda_T, \tag{6}$$

where $g_{5/2}(1) \approx 1.34$. For linear densities higher than $n_{c\perp}$, atoms accumulate in the transverse ground state, although no single quantum state is macroscopically occupied. The 3D interaction parameter at the onset of condensation for $T <$ 1 μK is $\rho_0 a^3 \lesssim 10^{-4}$, so that interactions have a negligible effect in this transition. On the other hand, the ratio $n_{c\perp}/n_t$ is of the order of $[(k_BT/\hbar\omega_\perp)(a/l_\perp)^{2/11}]^{11/6}$. For our experimental parameters, $(l_\perp/a)^{2/11} \simeq 1.9$, so that $n_{c\perp}/n_t \gg 1$ as soon as $k_BT/\hbar\omega_\perp \gtrsim 3$. Thus, one expects a quasicondensate in the transverse ground state to emerge immediately after the transverse condensation. As we see from Fig. 2, Eq. (6) and the MYYM prediction for n_1 are indeed in very good agreement with each other at high temperatures.

The transition width $(n_2 - n_1)/2(n_1 + n_2)$ is 0.6 in the 1D regime and decreases as the gas becomes more three dimensional. Deep in the 3D regime, n_2 lacks, however, physical meaning. As an example, for our experimental parameters and for $k_BT = 10\hbar\omega_\perp$, one expects only a small fraction of the atoms to be in the quasicondensate transverse mode at linear

density n_2 and one expects the fluctuations to actually exceed the quasicondensate prediction at higher densities [30]. We also note that, in the 1D limit, the Bogoliubov theory within the quasicondensate regime [31] predicts that the fluctuations are *increased* slightly when the density is *decreased*—a feature seen in the MYYM prediction [see Fig. 1(c)], but which is not resolved experimentally.

In Fig. 2, the change of the scaling of n_1 from $T^{2/3}$ [Eq. (5)] to $T^{5/2}$ [Eq. (6)] clearly reveals the dimensional crossover. This phase diagram depends, however, on the strength of interactions through the scattering length a. To investigate this dependence, we compute n_1 as a function of $k_B T/\hbar\omega_\perp$, for several values of $a/l_\perp$, using standard perturbation theory with respect to the 3D coupling $g_{3D} = 4\pi\hbar^2 a/m$, which correctly describes departures from the ideal-gas regime. For the parameters of our experiment, with $a/l_\perp \simeq 0.03$, this calculation (dashed-dotted curve in Fig. 2) is in qualitative agreement with the scaling from the 3D to the 1D regime. The disagreement with the data is mainly because for such a (large) value of $a/l_\perp$, interactions are not negligible even at linear densities smaller than n_1 [32]. If $a/l_\perp$ is decreased, the crossover toward the 3D behavior takes place at a higher temperature. More precisely, n_1 converges toward $n_{c\perp}$ when $n_{c\perp} \gg n_t$, i.e., when $k_B T/\hbar\omega \gg (a/l_\perp)^{-2/11}$. By fitting, for each $a/l_\perp$, the 1D and 3D asymptotic behavior with the scaling laws of Eqs. (5) and (6), respectively, we define the temperature of the dimensional crossover, $T_{\rm DC}$, as the point where these asymptotes intersect. The inset of Fig. 2 shows that $T_{\rm DC}$ scales as $(a/l_\perp)^{-2/11}$ as expected. We also see that $k_B T_{\rm DC}$ becomes significantly larger than $\hbar\omega_\perp$ only for extremely small values of $a/l_\perp$. In most experimental situations, however, $k_B T_{\rm DC} \sim \hbar\omega_\perp$, so that the transverse condensation leads immediately to the formation of a quasicondensate.

In conclusion, we have mapped out the quasicondensate transition throughout the 1D–3D dimensional crossover, for $k_B T/\hbar\omega_\perp$, ranging from 0.06 to 3.6. We have found that, whereas the transition is always governed by the 1D physics, it is activated by the degeneracy-driven transverse condensation in the 3D regime while it is interaction-driven in the 1D regime. An extension of this work would be to perform similar measurements in two-dimensional (2D) gases, characterizing the 2D–3D crossover and investigating the breakdown of the scale invariance [33,34]. For 1D gases, such measurements could also be used to investigate the crossover between the weakly and strongly interacting regimes. More generally, this work shows the power of fluctuation measurements as a test bed for competing theoretical models for the thermodynamic equation of state of a given physical system.

This work was supported by the IFRAF Institute, ANR Grant No. ANR-08-BLAN-0165-03, and by the Australian Research Council.

[1] D. S. Petrov, D. M. Gangardt, and G. Shlyapnikov, J. Phys. IV (France) **116**, 5 (2004).
[2] I. Bloch, J. Dalibard, and W. Zwerger, Rev. Mod. Phys. **80**, 885 (2008), and references therein.
[3] This phenomenon was introduced by N. J. van Druten and W. Ketterle, Phys. Rev. Lett. **79**, 549 (1997), for a system of finite longitudinal size, in which case the atoms eventually condense into the true ground state as the temperature is reduced.
[4] D. S. Petrov, G. V. Shlyapnikov, and J. T. M. Walraven, Phys. Rev. Lett. **85**, 3745 (2000).
[5] D. S. Petrov, G. V. Shlyapnikov, and J. T. M. Walraven, Phys. Rev. Lett. **87**, 050404 (2001).
[6] S. Dettmer *et al.*, Phys. Rev. Lett. **87**, 160406 (2001).
[7] F. Gerbier *et al.*, Phys. Rev. A **67**, 051602 (2003).
[8] J. Estève *et al.*, Phys. Rev. Lett. **96**, 130403 (2006).
[9] A. H. van Amerongen, J. J. P. Van Es, P. Wicke, K. V. Kheruntsyan, and N. J. van Druten, Phys. Rev. Lett. **100**, 090402 (2008).
[10] C. N. Yang and C. P. Yang, J. Math. Phys. **10**, 1115 (1969).
[11] K. K. Das, M. D. Girardeau, and E. M. Wright, Phys. Rev. Lett. **89**, 110402 (2002).
[12] G. E. Astrakharchik and S. Giorgini, Phys. Rev. A **66**, 053614 (2002).
[13] A. F. Ho, M. A. Cazalilla, and T. Giamarchi, Phys. Rev. Lett. **92**, 130405 (2004).
[14] U. Al Khawaja, N. P. Proukakis, J. O. Andersen, M. W. J. Romans, and H. T. Stoof, Phys. Rev. A **68**, 043603 (2003).
[15] A. Görlitz *et al.*, Phys. Rev. Lett. **87**, 130402 (2001).
[16] T. Stöferle, H. Moritz, C. Schori, M. Kohl, and T. Esslinger, Phys. Rev. Lett. **92**, 130403 (2004).
[17] J. Armijo, T. Jacqmin, K. V. Kheruntsyan, and I. Bouchoule, Phys. Rev. Lett. **105**, 230402 (2010).
[18] K. V. Kheruntsyan, D. M. Ganghardt, P. D. Drummond, and G. V. Shlyapnikov, Phys. Rev. A **71**, 053615 (2005).
[19] J. N. Fuchs, X. Leyronas, and R. Combescot, Phys. Rev. A **68**, 043610 (2003); A. Muñoz Mateo and V. Delgado, *ibid.* **77**, 013617 (2008).
[20] S. Manz *et al.*, Phys. Rev. A **81**, 031610 (2010).
[21] T. Müller *et al.*, Phys. Rev. Lett. **105**, 040401 (2010).
[22] C. Sanner *et al.*, Phys. Rev. Lett. **105**, 040402 (2010).
[23] J. Estève *et al.*, Phys. Rev. A **70**, 043629 (2004).
[24] K. V. Kheruntsyan, D. M. Gangardt, and P. D. Drummond, Rev. Lett. **91**, 040403 (2003).
[25] I. Bouchoule, N. J. Van Druten, and C. I. Westbrook, in *Atom Chips*, edited by J. Reichel and V. Vuletic (Wiley, Berlin, 2011).
[26] M. Olshanii, Phys. Rev. Lett. **81**, 938 (1998).
[27] I. Bouchoule, K. V. Kheruntsyan, and G. V. Shlyapnikov, Phys. Rev. A **75**, 031606 (2007).
[28] T the weak interaction condition $\gamma = mg/\hbar^2 n_t \ll 1$ gives $(mT/\hbar^2 n_t^2) \ll 1$, confirming that the gas is degenerate.
[29] $n_{c\perp}$ is obtained from Eq. (2) by taking the limit $k_B T/\hbar\omega_\perp \to \infty$ and then $\mu \to 0$.
[30] For smaller a and/or higher T, one can even have $n_2 < n_1$.
[31] C. Mora and Y. Castin, Phys. Rev. A **67**, 053615 (2003).
[32] For smaller values of $a/l_\perp$, the perturbative calculation shows much better agreement with both the scaling law of n_t in the 1D regime and with $n_{c\perp}$ in the 3D regime.
[33] S. P. Rath *et al.*, Phys. Rev. A **82**, 013609 (2010).
[34] C.-L. Hung, X. Zhang, N. Gemelke, and C. Chin, e-print arXiv:1009.0016.